CSMA 2022
15ème Colloque National en Calcul des Structures
16-20 Mai 2022, Presqu'île de Giens (Var)

Preprint: Towards a reproducible research in topological optimization of aerostructures

J. Morlier[1], V. Bhat[1], E. Duriez[1], M. Charlotte[1]

[1] *ICA, Université de Toulouse, ISAE-SUPAERO, MINES ALBI, UPS, INSA, CNRS, Toulouse, France, {joseph.morlier,vilas.bhat,edouard.duriez,miguel.charlotte}@isae-supaero.fr*

Résumé — This paper attempts to demonstrate the contribution of reproducible research with two recent attempts at the ICA entitled GGP [S. Coniglio S *et al.* (2020),"Generalized geometry projection : a unifed approach for geometric feature based topology optimization". Arch. Comput. Methods in Eng., (2020), vol. 27, pp. 1573-1610] and EMTO [E. Duriez *et al.* (2021), "A well connected, locally-oriented and efficient multi-scale topology optimization (EMTO) strategy". Structural and Multidisciplinary Optimization, pp. 1-24]. The first method standardizes the existing methods in explicit topological optimization. The second offers a multiscale topological optimization environment. The common point : Two basic articles with the associated code top99 and top88 (Matlab) ; initiative of the DTU. The comparison of these methods on the optimization of an airplane wing rib (2D) highlights their complementarity, with one giving a simple concept, the other one giving a micro-architectural design whose manufacture must be automated.

Mots clés — Topology optimization, geometric projection, reproducible research.

1 Introduction

Structural engineers always design a load bearing structure with two important parameters in mind. One being "How best to design without compromising on safety and operational requirements ?", the other being "How to make it the lightest ?", which directly translates to obtaining the best performing structure with the least weight possible. This is precisely the question tackled by structural optimization, which aims to find an optimum material distribution for a specified load under a specific set of constraints and boundary conditions.

The landmark paper from Bendsøe and Kikuchi [1], and later by Zhou and Rozvany [2] set off a renewed flurry of investigative work in academics to exploit and provide alternatives to this numerical homogenization method, named Solid Isotropic Material with Penalization (SIMP), that essentially uses a power law to restrict material densities to either 0 or 1.

Concurrently a method influenced by the natural evolution of structures observed in nature inspired a new method named Evolutionary Structural Optimization [ESO] [3] where elements are progressively removed using a Rejection Criterion that employs, for example, a minimum von Mises stress criterion, and repeated until a desired optimum is reached. Other notable and proven methods include the level set method [4] and its extension that includes classical shape derivatives on a fixed Eulerian mesh [5], topology optimization using Topology Description Function (TDF) [6].

Several drawbacks of density or pixel based topology optimizations have been noted, the most deleterious being the number of variables. An FEA model with more than 1 million pixel/voxel elements results in an optimization problem with similar number of variables, leading to enormous computational cost that effectively delays the early adoption of topology optimization methodologies. Another drawback is the lack of explicit control over design features like minimum length or breadth of the members in the solutions formed, or to enforce the presence or absence of voids and more, along with the absence of a clear boundary of the solution being formed primarily due to the presence of gray areas that are subject to further understanding and post-processing. Currently for SIMP, it is enforced using the purely heuristic method of filtering. To overcome these drawbacks, multiple projection based methods using structural/geometrical components were proposed.

This paper will attempt to synthesize the advances in explicit topological optimization in the unified

opensource framework GGP. Section 2 will present the existing geometric projection methods. Section 3 will introduce the unified method and its implementation. Section 4 will define the aerostructures testcase and a benchmark of methodologies (GGP-EMTO-SIMP) all opensource.

2 Geometric Projection methods

The first among such methods was the Moving Morphable Components (MMC) [7], improved upon in [8], which projects the TDF of the components onto the Eulerian grid. The characteristics of components in this framework can be changed according to the required fidelity of the solution expected, which can vary from a round ended component, components with varying thicknesses to component with curved skeletons [9]. A noteworthy variation of the above given method is the Method of Moving Void (MMV) [10]), where B-spline surfaces or curves, instead of structural bars, are projected onto Eulerian meshes to indicate the absence of material. Multiple applications of topology optimization using the MMC framework have already been published.

Yet another projection method was introduced by Bell et. al., called the Geometric Projection (GP) [11], that finds the optimum layout of linearly elastic rectangular-shaped bars of fixed width and thickness to obtain the stiffest structure possible. This method was elaborated to obtain a complete framework in [12], which used round ended bars of fixed width, and varying size per component to indicate a fraction of a solid material anywhere in the design space. Recently, the bar like structural components in the original GP framework has been replaced by supershapes by [13] that promises higher fidelity in terms of shapes achieved compared to simple bars or plates.

Parallelly, a projection method that used mass nodes as its building blocks of solution instead of structural members or geometric shapes was proposed in an approach called Moving Node Approach (MNA) by Overvelde [14], which received relatively less attention than the other two methods presented above. This method computes each FE elements' center point with respect to the local co-ordinates in each component vector over which the weighing functions are directly applied to the local variable to obtain the local density. A variation of this method has been developed with a mesh-free approach in [15] and more recently used to compute optimized structural solutions subject to 3D printing [16].

Recently, all major explicit approaches for topology optimization (i.e., MMC, GP & MNA) were assimilated in a general framework, named Generalized Geometric Projection or GGP in [17]. Finally, a review of geometric projection methods is presented in [18], called feature mapping methods, that discuss the choices available to accomplish mapping of high level geometric parameters onto a fixed mesh and combination of geometric primitives. In this work, it was demonstrated how all explicit methods differed from one another in the method by which the geometric primitives were projected onto the design space. This framework is detailed in next sections, along with comparative results against solutions from the SIMP method.

3 GGP Framework

The first opensource top99 [19] established in 2001 a state of the art 2D topology optimization framework (Matlab). It contains in 99 lines matlab code ; a FEA solver (using QUAD element), an optimizer (Heuristic) and post processing treatment. It has been vectorized for efficiency in top88 [20] then extended to 3D [21] and again optimized with high performance computing in top99neo [22]. The interested reader have a list and abstract of interesting educational papers in [23]. These codes are used as a basis of the GGP project and also used in SUPAERO classrooms. The code is opensource and available on Matlab, Python and Julia (`https://topggp.github.io/blog/`) with a recent extension to 3D printing [24].

The following section outlines the GGP framework required to understand the problem formulation, that varies depending upon the application. An example in structural compliance minimisation is explained in detail in the next section. The GGP version of MMC, MNA, and GP will be called respectively AMMC, AMNA and AGP and are explained in details in [17].

3.1 Generalized Geometric Projection (GGP) formulation

The solution in the *GGP* framework comprises of round ended bars for geometric primitives, each having 6 variables (coordinate position X and Y, length L, width H, inclination angle θ and size (or mass) m), illustrated in figure 1. Its characteristic function Υ, which defines the density inside the primitive is given by :

FIGURE 1 – Example component schematic

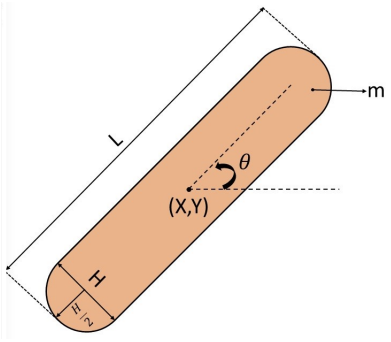

$$\Upsilon(\{X_g\},\omega_i) = \begin{cases} 1 & \text{if } \{X_g\} \in \omega_i \\ 0 & \text{otherwise} \end{cases} \tag{1}$$

Where $\{X_g\}$ is the design domain and ω_i is the geometric primitive. It must be acknowledged that the geometric primitives do not define this framework, but rather the formulation which potentially gives rise to the 3 methods that will be explained in the following sections. These geometrical primitives are used to update a fixed mesh finite element model by projection and boolean operations. Next, the local density formulation, considered as an estimation of weighted volume fraction, is used for the projection, given by :

$$\begin{aligned} \delta_i^{el} &= \frac{\int_{D(\{X_g^{el}\},p,R)} W_i(\{X\},\{X_i\},\{r\}) d\Omega}{\int_{D(\{X_g^{el}\},p,R)} d\Omega} \\ &\approx \frac{\sum_{k=1}^{N_{gp}} \varphi_k W_{ik}}{\sum_{k=1}^{N_{gp}} \varphi_k} \end{aligned} \tag{2}$$

Where $W_i(\{X\},\{X_i\},\{r\})$ is a regular continuous approximation of $\Upsilon(\{X_g\},\omega_i)$, $\{r\}$ is a vector of hyper parameters that controls the length scale of the transition of W_i in [0,1], W_{ik} is equal to the characteristic function value at Gauss point location and φ_k are integration weights. The evaluation of δ_i^{el} using Gauss quadrature is given using the second equation in (2). Using the notation of $\{\delta^{el}\}_v$ and $\{\delta^{el}\}_c$, described as the vector of local volume fractions computed using density characteristic function W_v and W_c respectively in the el^{th} element centroid, the final step involves updating the fixed mesh of the FE model using the expression

$$\begin{aligned} E^{el} &= \mathbb{M}(\{\delta^{el}\}_c, E, E_{min}, \kappa) \\ \rho^{el} &= \mathbb{V}(\{\delta^{el}\}_c, \kappa) \end{aligned} \tag{3}$$

Where $\mathbb{M}$ and $\mathbb{V}$ are functions that provide the Young's Modulus and the Volume fractions of each finite element as the resultant of being within a geometric primitive boundary. Subsequently, the method of calculation of Young's modulus and element density depends on the method chosen.

3.2 Specific Formulation

With the GGP framework discussed in brief, the exact formulation will now be explained. The objective functions will be mentioned and discussed on a case by case basis in a later section of this article. For

the sake of completeness the most common objective, i.e., to minimize the compliance of the resulting structure, will be used. We have

$$\begin{cases} \min_{\{x\}} C = \{U\}^T \{F\} \\ s.t \\ V = \frac{\sum_{el=1}^{N} \rho^{el}}{N} \leq V_0 \\ \{l_b\} \leq \{x\} \leq \{u_b\} \end{cases} \tag{4}$$

Where $\{x\}$ is the design vector to be determined that consists of variables of the geometric primitive, $\{l_b\}$ and $\{u_b\}$ is its lower and upper bound respectively, $\{F\}$ is a vector composed of external imposed loads on the design space, C is the compliance of the resulting structure, $\{U\}$ is a vector of nodal displacements, V_0 is the maximum volume fraction allowed, N is the total number of elements and ρ^{el} is the density of a given element in the design space. The displacement U is obtained using the static force balance equation given by :

$$[K]\{U\} = \{F\} \tag{5}$$

$$\text{and therefore} \quad \{U\} = [K]^{-1}\{F\} \tag{6}$$

Where $[K]$ is the assembled global stiffness matrix. The global design space is discretized into a N number of solid elements with unit thickness, over which the geometric primitives are arranged and project their topology. From the finite element theory :

$$[K] = \bigoplus_{el=1}^{N} [K^{el}] \tag{7}$$

$$\text{where} \quad [K^{el}] = E^{el}[K_0] \tag{8}$$

Where $[K^{el}]$ is the elementary stiffness matrix, $[K_0]$ is the 8×8 stiffness matrix of a $dx \times dx$ plane stressed solid element, and $[K]$ is the assembled global stiffness matrix. It must be highlighted that $[K]$ must be a non singular matrix, and therefore future formulations that lead to the stiffness matrix assembly must be considered with careful attention. The geometric primitives (and hence the design variables) are discussed in the previous section.

To avoid the singularity of $[K]$ matrix, which is dependent on the density ρ^{el}, the notation provided by Bendsoe and Kikuchi in the SIMP methodology [1] is used :

$$E^{el} = E_{min} + (E - E_{min})\rho^p \tag{9}$$

Where E^{el} is the element Young's modulus, E_{min} is a minimum sufficient to avoid singularities and ρ is the density penalized using the parameter p. This ensures that the design obtained is fairly 0/1 density field, rather than consisting of a broad range of densities in [0,1]. It is now necessary to investigate methods to obtain the value of density ρ, the expressions for which is dependent on the method chosen in the framework, and is discussed later.

Let us begin by referring to d as the radial distance of each components' center $\{X,Y\}^T$ to its boundary $\partial\omega$, and let ω be the area of the components. The term d is calculated by :

$$d = \begin{cases} \sqrt{\frac{h^2}{4} - \frac{L^2 \sin\phi^2}{4}} + \frac{L}{2}|\cos\phi| & \text{if } \cos\phi^2 \geq \frac{L^2}{L^2+h^2}, \\ \frac{h}{2|\sin\phi|} & \text{otherwise.} \end{cases} \tag{10}$$

The region of influence due to the projected geometries is a function of the FE elements' distance from the component centers. If the centre co-ordinates of a FE i is denoted by (x_i, y_i), then the polar coordinates $\{\rho_i, \phi_i\}$ is defined by :

$$\rho_i = \sqrt{(x_i - X)^2 + (y_i - Y)^2} \tag{11}$$

$$\phi_i = \begin{cases} \arctan\left(\frac{y_i - Y}{x_i - X}\right) - \theta & \text{if } x \neq X \\ \frac{\pi}{2}\text{sign}(y - Y) - \theta & \text{otherwise} \end{cases} \tag{12}$$

The distance from a FE element i to the component medial axis, expressed as υ, which is expressed in terms of ρ_i and ϕ_i :

$$\upsilon = \begin{cases} \sqrt{\rho^2 + \frac{L^2}{4} - \rho L |\cos\phi|} & \text{if } \rho^2 \cos\phi^2 \geq \frac{L^2}{4}, \\ \rho |\sin\phi| & \text{otherwise} \end{cases} \tag{13}$$

Having known the region of influence over the whole design space, the characteristic function value W is given by the method chosen in the framework, i.e., AMMC, AMNA or AGP. The summary of all the parameters and variables to be used in GGP to recover the original methods discussed is mentioned in Table 1. The readers are suggested to refer to [17] for a thorough description of all the functions mentioned above, along with its sensitivity analysis.

TABLE 1 – Choice to be made to recover all other approaches using Generalized Geometric Projection

Method	MMC	GP	MNA
W^c	$H_\varepsilon(\chi^{el})^q$	$\tilde{\delta}_i^{el} m_i^{\gamma_c}$	$m_i^{\gamma_c} w_i^{el}$
W^v	$H_\varepsilon(\chi^{el})$	$\tilde{\delta}_i^{el} m_i^{\gamma_v}$	$m_i^{\gamma_v} w_i^{el}$
p	∞	∞	∞
R	$\frac{\sqrt{3}}{2}dx$	$\frac{1}{2}dx$	$\frac{1}{2}dx$
N_{GP}	4	1	1
$\mathbb{V}$	$\frac{\sum_{j=1}^4 H_\varepsilon(\chi_j^{el})}{4}$	$\Pi(\hat{\delta}_v^{el}, \kappa)$	$\Pi(\delta^{el}{}_v, \kappa)$
$\mathbb{M}$	$\frac{\sum_{j=1}^4 (H_\varepsilon(\chi_j^{el}))^q}{4}$	$\Pi(\hat{\delta}_c^{el}, \kappa)E$	$E_{min} + (E - E_{min})\Pi(\delta^{el}{}_c, \kappa)^{p_b}$

4 Results and discussion

4.1 Wing Rib test case

As a final application, the more complex problem of the wing rib design is considered here. A section of 15% to 70% is chosen from the Eppler 402 airfoil. Realistically speaking, a wing rib must be designed considering multiple load cases (6-12 load cases for the leading edge rib alone, in [25]), which includes shear loads, buckling, torsion and more. Due to the aim of the article being to measure the performance and feasibility of GGP and SIMP, only the uniform pressure loads over the wing ribs are imposed as shown in Figure 2. Moreover no buckling or stress based topology optimization has been conducted.

The objective of the optimization problem is compliance minimization.

FIGURE 2 – Design domain and boundary condition for the Wing Rib problem

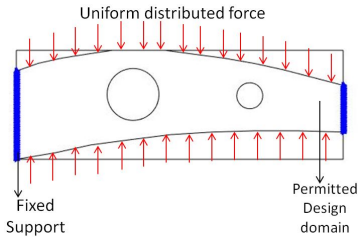

4.2 Results for several (low) Volfrac i.e. exploration of the design domain

For all tests in this paper, the initial component pattern X0 is shown in Fig 3.

The resultant objective achieved are shown in Table 2. The numerical Design of experiments offered here is a 4x4 analysis (4 method, 4 volume fraction, same X0). It is important to notice that the results

FIGURE 3 – Initial component distribution for Rib problem

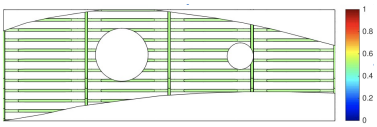

(gradient based) are dependent of the X0 and we probably get stuck in a local minimum (Red deviation in 2). We are comparing only AGP and AMNA.

Method	Parameters	Volume Fraction			
		0.3	0.4	0.5	0.6
SIMP	Objective	0.4332	0.2719	0.1975	0.1549
AGP	Objective	0.296	0.206	0.165	0.137
	Deviation	31.6%	24.31%	16.3%	11.5%
AMNA	Objective	0.756	0.293	0.194	0.15
	Deviation	74.5%	7.94%	1.67%	3.49%

TABLE 2 – Compliance values for a Wing Rib with uniformly distributed force

The comparison reflects that : The AGP method provides the best performance, while the solution from AMNA method partially reflects the wing rib structures currently in use. Let's have a closer look to the results of GGP at Volfrac=0.3. The two methods give two differents topologies, AGP being the better than the SIMP reference. The only difference is the hyperparameters of the method (same X0, same stopping criteria i.e. KKT conditions, same grid for analysis).

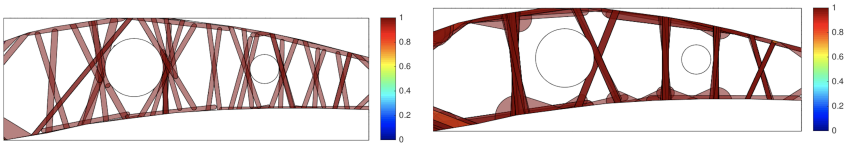

(a) AGP Component (b) AMNA Component

FIGURE 4 – GGP comparison at Volfrac=0.3

4.3 Comparison with EMTO

The results are obtained here for Volfrac=0.5.The multiscale methodology is detailled in [26] and the code is given at `https://github.com/mid2SUPAERO/EMTO`. The comparison gives :

— Cagp=0.194
— Cemto=0.172 (homogenized)
— Csimp=0.198

The multiscale approach is a complete *redesign* : it creates multiple paths for internal forces (and the fabrication needs to be automated) whereas GGP allows *easy interpretation* and exploration of potential design structures with explicit components and so shortcut the CAD-CAE path. The two methods are fast and complementary and the two codes are available on github.

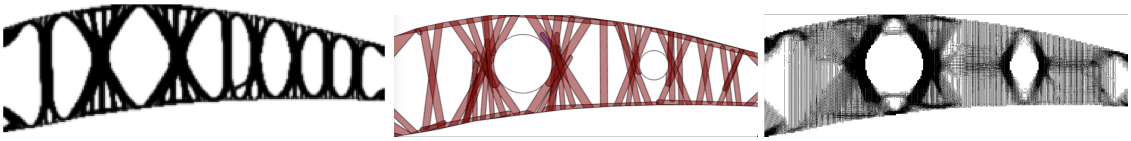

(a) SIMP (b) AGP Components (c) EMTO

FIGURE 5 – SIMP vs GGP-MNA vs EMTO at volfrac=0.5

5 Conclusions

Exploring potential design of structures is a complex task. GGP unified framework can really help the structural engineers by providing explicit assembly of geometric features computed using three different methods in the same code. We provide in this paper an aerostructures testcase and resulting solutions to the SIMP and EMTO methodology. All the code are opensource and will help the interesting reader to reproduce our results.

Acknowledgment

The authors would like to thank the ISAE Fondation Class Gift Promo '83 for funding the post of Research Assistant and AMX fund for supporting Edouard's PhD. Both made this article and other associated works possible. The main author wants also to thanks all colleagues and students (MsC, PhD) which have worked on the topGGP project : S. Coniglio, C. Gogu, G. Capasso, J. Cruz-Ferreira-Matos, R. Grapin. On part of this work is teached at SUPAERO and available at `https://github.com/jomorlier/mdocourse`

Références

[1] Martin Philip Bendsøe and Noboru Kikuchi. Generating optimal topologies in structural design using a homogenization method. *Computer methods in applied mechanics and engineering*, 71(2) :197–224, 1988.

[2] M Zhou and GIN Rozvany. The coc algorithm, part ii : Topological, geometrical and generalized shape optimization. *Computer methods in applied mechanics and engineering*, 89(1-3) :309–336, 1991.

[3] Yi M Xie and Grant P Steven. A simple evolutionary procedure for structural optimization. *Computers & structures*, 49(5) :885–896, 1993.

[4] Michael Yu Wang, Xiaoming Wang, and Dongming Guo. A level set method for structural topology optimization. *Computer methods in applied mechanics and engineering*, 192(1-2) :227–246, 2003.

[5] Grégoire Allaire, François Jouve, and Anca-Maria Toader. Structural optimization using sensitivity analysis and a level-set method. *Journal of computational physics*, 194(1) :363–393, 2004.

[6] MJ De Ruiter and F Van Keulen. Topology optimization using a topology description function. *Structural and Multidisciplinary Optimization*, 26(6) :406–416, 2004.

[7] Xu Guo, Weisheng Zhang, and Wenliang Zhong. Doing topology optimization explicitly and geometrically—a new moving morphable components based framework. *Journal of Applied Mechanics*, 81(8), 2014.

[8] Weisheng Zhang, Jie Yuan, Jian Zhang, and Xu Guo. A new topology optimization approach based on moving morphable components (mmc) and the ersatz material model. *Structural and Multidisciplinary Optimization*, 53(6) :1243–1260, 2016.

[9] Xu Guo, Weisheng Zhang, Jian Zhang, and Jie Yuan. Explicit structural topology optimization based on moving morphable components (mmc) with curved skeletons. *Computer methods in applied mechanics and engineering*, 310 :711–748, 2016.

[10] Weisheng Zhang, Jishun Chen, Xuefeng Zhu, Jianhua Zhou, Dingchuan Xue, Xin Lei, and Xu Guo. Explicit three dimensional topology optimization via moving morphable void (mmv) approach. *Computer Methods in Applied Mechanics and Engineering*, 322 :590–614, 2017.

[11] Bryan Bell, Julian Norato, and Daniel Tortorelli. A geometry projection method for continuum-based topology optimization of structures. In *12th AIAA Aviation Technology, integration, and*

operations (ATIO) conference and 14th AIAA/ISSMO multidisciplinary analysis and optimization conference, page 5485, 2012.

[12] JA Norato, BK Bell, and Daniel A Tortorelli. A geometry projection method for continuum-based topology optimization with discrete elements. *Computer Methods in Applied Mechanics and Engineering*, 293 :306–327, 2015.

[13] Julián A Norato. Topology optimization with supershapes. *Structural and Multidisciplinary Optimization*, 58(2) :415–434, 2018.

[14] Johannes TB Overvelde. The moving node approach in topology optimization. *Master thesis*, 2012.

[15] Ghislain Raze, M Charlotte, and Joseph Morlier. Optimisation topologique sans maillage-vers la reconnaissance d'éléments structuraux. In *13e colloque national en calcul des structures*, 2017.

[16] Vilasraj K Bhat, Simone Coniglio, Joseph Morlier, and Miguel Charlotte. Une approche par projection pour l'optimisation topologique de structures imprimées par fabrication additive. In *14e colloque national en calcul des structures*, 2019.

[17] Simone Coniglio, Joseph Morlier, Christian Gogu, and Rémi Amargier. Generalized geometry projection : A unified approach for geometric feature based topology optimization. *Archives of Computational Methods in Engineering*, 27 :1573–1610, 2020.

[18] Fabian Wein, Peter D Dunning, and Julián A Norato. A review on feature-mapping methods for structural optimization. *Structural and multidisciplinary optimization*, pages 1–42, 2020.

[19] Ole Sigmund. A 99 line topology optimization code written in matlab. *Structural and multidisciplinary optimization*, 21(2) :120–127, 2001.

[20] Erik Andreassen, Anders Clausen, Mattias Schevenels, Boyan S Lazarov, and Ole Sigmund. Efficient topology optimization in matlab using 88 lines of code. *Structural and Multidisciplinary Optimization*, 43(1) :1–16, 2011.

[21] Kai Liu and Andrés Tovar. An efficient 3d topology optimization code written in matlab. *Structural and Multidisciplinary Optimization*, 50(6) :1175–1196, 2014.

[22] Federico Ferrari and Ole Sigmund. A new generation 99 line matlab code for compliance topology optimization and its extension to 3d. *Structural and Multidisciplinary Optimization*, 62(4) :2211–2228, 2020.

[23] Chao Wang, Zhi Zhao, Ming Zhou, Ole Sigmund, and Xiaojia Shelly Zhang. A comprehensive review of educational articles on structural and multidisciplinary optimization. *Structural and Multidisciplinary Optimization*, pages 1–54, 2021.

[24] Krishnaraj Vilasraj Bhat, Gabriele Capasso, Simone Coniglio, Joseph Morlier, and Christian Gogu. On some applications of generalized geometric projection to optimal 3d printing. *Computers & Graphics*, 2021.

[25] Lars Krog, Alastair Tucker, Gerrit Rollema, et al. Application of topology, sizing and shape optimization methods to optimal design of aircraft components. In *Proc. 3rd Altair UK HyperWorks users conference*, 2002.

[26] Edouard Duriez, Joseph Morlier, Miguel Charlotte, and Catherine Azzaro-Pantel. A well connected, locally-oriented and efficient multi-scale topology optimization (emto) strategy. *Structural and Multidisciplinary Optimization*, pages 1–24, 2021.